Self-organized pattern formation in the oxidation of supported iron thin films. I. An experimental study

S. R. Shinde,[1,*] Abhijit S. Ogale,[1] S. B. Ogale,[1,2,†] S. Aggarwal,[2] V. Novikov,[1,‡] E. D. Williams,[1] and R. Ramesh[1,2]
[1]*Department of Physics, University of Maryland, College Park, Maryland 20742*
[2]*Department of Materials and Nuclear Engineering, University of Maryland, College Park, Maryland 20742*
(Received 16 October 2000; revised manuscript received 1 February 2001; published 21 June 2001)

The evolution of patterned morphology during thermal oxidation of a supported metal thin film is examined as a case of strained reaction-diffusion system; the strain originates from the large density difference between the oxide and the metal. In the moderate temperature regime, where bulk diffusion is weak, the pattern reflects the length scale of the original metal film grain structure, with local features characteristic of self-organized chemical microreactors, as well as large scale polygonal surface undulations presumably caused by stress accommodation. At higher temperature, where bulk diffusion is brisk, the process of Ostwald ripening strongly reforms the morphology formed at lower temperature, and leads to distributed spiral-type configurations. These observations and analysis are supported by a simulation study reported in the accompanying paper II by Abhijit S. Ogale [Phys. Rev. B **64**, 035409 (2001)]

DOI: 10.1103/PhysRevB.64.035408 PACS number(s): 68.65.−k, 81.15.−z

I. INTRODUCTION

Development of self-organized patterns and textures in natural systems has always been an exciting field of research inquiry due to its obvious aesthetic appeal, and the challenge it poses for identification of unifying principles underlying such phenomena.[1,2] Understanding the process of self-organization has become all the more important in recent times in view of its direct significance in the context of the rapidly developing field of nanotechnology, which aims for self-assembly to achieve higher device packing densities and responses emerging from quantum size effects.[3–5]

Recently Aggarwal *et al.*[6] demonstrated that oxidation of supported metal films can lead to a fairly uniform self-assembly of metal-oxide hillock patterns. Generically, this is a case of a reaction-diffusion system evolving under the internal stress caused by the significant density difference between the metal and its oxide(s). Since oxides offer a rich and wide variety of electrical, structural, magnetic and optical property options, controlled self-organized growth of such structures has significant application potential to future electronic, optoelectronic, and spintronic devices. However, in order to control and possibly tune the pattern formation in this or similar cases, a deeper understanding of the participating processes is essential. In this and the accompanying paper by Ogale,[7] we address some key issues in this context.

II. EXPERIMENTAL

Here we study the oxidation of Fe films as a representative case, although similar pattern formation is observed in other metal films as well. Fe films were deposited on single-crystal $SrTiO_3(100)$ substrates by pulsed laser deposition (PLD). The KrF excimer laser ($\lambda = 248$ nm) was employed for the ablation of Fe target and the depositions were performed in vacuum (2×10^{-6} Torr). The laser fluence and the substrate temperature were kept at 2.5 J/cm^2 and 30 °C, respectively. Typically, data for films with thickness of ~500 Å are analyzed in this paper, although the thickness dependence of pattern formation is also given. After deposition, the films were oxidized by *ex situ* annealing in flowing oxygen at temperatures ranging from 500 to 1050 °C for different durations. The rate of heating (cooling) was 20 °C/min (10 °C/min) in all cases.

III. RESULTS AND DISCUSSION

In Fig. 1 are shown atomic force microscopy (AFM) images of the morphologies obtained for oxidized films. The morphology at all temperatures below 950 °C exhibits local surface undulations wrapped by an irregular polygon pattern, as in Figs. 1(a) and 1(b). The surface elevation is about 20 nm higher on the polygon edges as compared to that within the polygon area. At temperatures above ~1000 °C, separate hillocks begin to get defined. In Fig. 1(c), which corresponds to a hold time of 10 s at 1050 °C, one observes a high density of small elongated hillocks, with fracture lines cutting across. A further increase in the duration of the high-temperature treatment leads to the development of a necklike labyrinth geometry [Fig. 1(d)] and finally, disappearance of necks leading to a greatly improved definition of individual hillocks [Fig. 1(e)]. These hillocks are isolated from each other and there is no connectivity in the film. It should also be noted here that these hillocks are arranged in a spiral coordination. In Fig. 1(e), it can also be seen that some hillocks are brighter in contrast than others, indicating that they are taller than the rest. Height analysis shows that these are over ~150 nm in height, and when the shorter ones are filtered out, the pattern appears as shown in Fig. 1(f). Interestingly, this pattern is polygonal and resembles the patterns of Figs. 1(a) and 1(b) in appearance and length scale. Similar patterns are also found by height filtering performed on the images in Figs. 1(c) and 1(d) as well.

We performed fast Fourier transform (FFT) analysis on all the patterns in Fig. 1 and the results are shown in Fig. 2. The curve identification (a)–(f) in Fig. 2, corresponds to the patterns of Fig. 1. It can be seen that the curves *a*, *b*, and *c* are bimodal, representing one short (broad peak located at large $q\sim3.5\ \mu m^{-1}$) and one long (sharp feature at very small

 ©2001 The American Physical Society

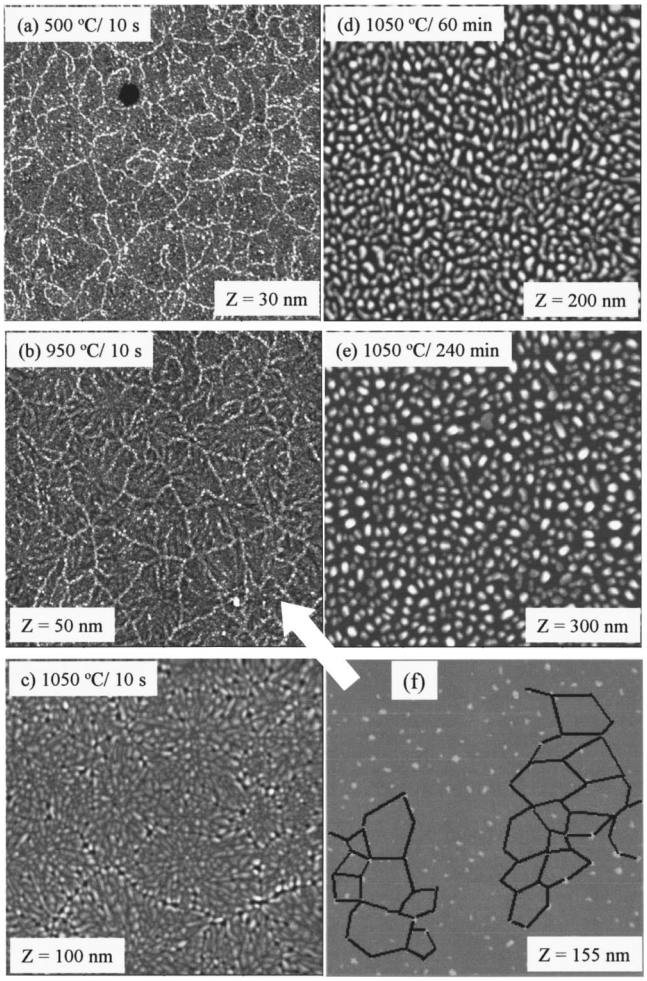

FIG. 1. (a)–(f) AFM images ($10\times10\ \mu m^2$) of 500 Å Fe films oxidized at different temperatures and durations. The contrast in the image corresponds to different heights of the film surface: full white representing the highest elevation and full black representing the substrate. The Z range used for each AFM scan is given in respective image. Figure (f) is obtained by filtering out the features below a height of ~150 nm. The line coordinations of these are also shown.

$q\sim0.3$–$0.6\ \mu m^{-1}$) length scale in the pattern. The feature at small q is present in curves d and e also, and is not clearly discernable because of the low statistics on the small image frame. The fact that it is present is, however, clear from curve (f) which represents the pattern of the taller hillocks in Fig. 1(e). The sharp peak in these curves reflects the length scale of the polygons observed in Figs. 1(a) and 1(b) and also the spread of the spiral in Fig. 1(f). As we shall see, the large q feature is due to the grain structure in the film.

The transforms in Fig. 2 reveal sharpening of the large q feature with increase in temperature, but its weight starts shifting to lower q only at temperatures above ~1000 °C. The sharpening reflects local organization, as in chemical microreactors.[8] The shift to lower q implies increased mean separation between individual hillocks (grains), which in turn implies ripening or coarsening. Interestingly, the position of the small q feature is roughly fixed, suggesting that the long length scale, which evolves during early stages, continues to hold in place for the entire pattern formation process.

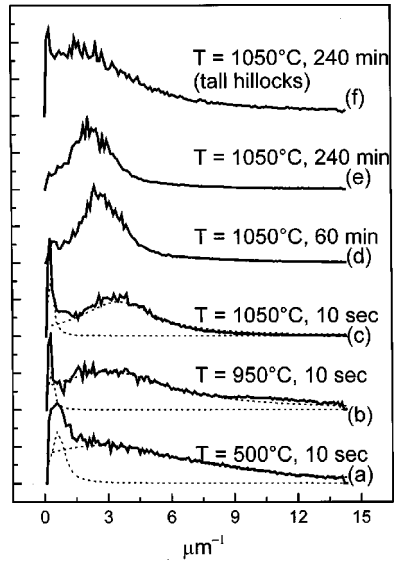

FIG. 2. The curves (a)–(f) represent the fast Fourier transforms corresponding to patterns (a)–(f) of Fig. 1. The successive curves are shifted along the y axis for clarity.

In Fig. 3 we show the bearing analysis for some of the patterns shown in Fig. 1. The height distribution sharply changes near the highest oxidation temperature of ~1000 °C. The amplitude of surface undulations also changes from ~10–20 nm to over 100 nm. In the inset of Fig. 3, we give the estimated bulk diffusion length for Fe in its oxide as a function of temperature for different times. The length increases dramatically above ~1000 °C. The fact that ripening of hillocks occurs above this temperature implies the role of bulk diffusion in this process and points to Ostwald ripening.

It is important to mention here that the morphological features and their development reported for iron films subjected to oxidation were *not* observed for iron oxide films grown by PLD and then subjected to a comparable treatment.

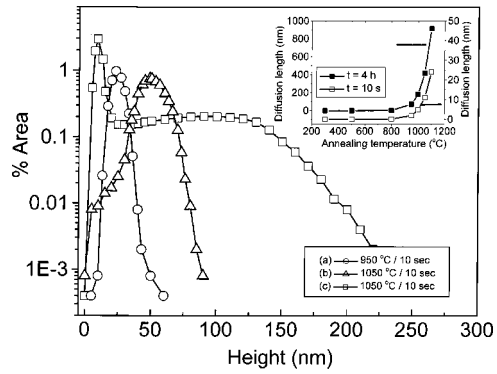

FIG. 3. Bearing analysis curves highlighting the changes in the film morphology as the annealing temperature and the duration are raised. Each point on the curve shows the fraction of the film in the imaginary plane drawn at corresponding height above the substrate. The inset shows diffusion length as a function of temperature and annealing duration (Ref. 12).

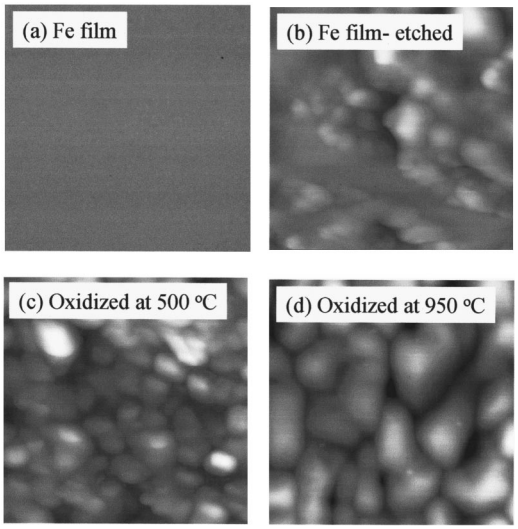

FIG. 4. AFM images ($500\times500\,\mathrm{nm}^2$) of (a) as-deposited Fe film, (b) as-deposited film subjected to acid etch to expose grains, (c) as-deposited film oxidized at 500 °C, and (d) as-deposited film oxidized at 950 °C.

This clearly suggests the importance of the chemical reaction to form the oxide and the resulting evolving oxidative stress (caused by the large density difference between the metal and its oxide) in the pattern formation process. In the present case the relevant densities in gm/cm^3 are 7.86 (Fe), 5.972 (FeO), 5.197 (Fe_3O_4), and 5.27 (α-Fe_2O_3).

We also address the obvious question of the possible role of grain boundaries in the process of initial oxidation. We used an acid etch to expose the grain boundaries in the as-deposited Fe film. AFM pictures of the as-deposited and etched Fe films are shown in Figs. 4(a) and 4(b), respectively. In Figs. 4(c) and 4(d) we also reproduce the patterns of Figs. 1(a) and 1(b) at the same length scale. The fact that a flat film, as in Fig. 4(a), grows features as in Fig. 4(c), which are similar to the grain-boundary features in Fig. 4(b), suggests that initial oxidation does occur near grain boundaries. At higher temperature of 950 °C, ripening is clearly seen to occur. Note, however, that these are the small scale structures in the patterns that are represented by the large q feature in the FFT spectra. The large scale structures, such as the polygonal patterns or the spirals, are not directly related to grain-boundary structures.

We first discuss the patterns formed when the highest oxidation temperature is less than ~1000 °C. At such temperatures, the oxidation proceeds along the grain-boundary network, and strong compressive stresses develop in the surrounding regions due to the large density difference between the oxide and the metal. The resulting stress fields propagate out at the velocity of sound. Such fields, originating from different random line sources, would interfere, causing inhomogeneous surface stress distribution, and thereby promoting morphological instability.[9–11] The polygonal distribution of surface undulations is a signature of such an instability on a long length scale. The early local growth of oxide in our case may also reflect the character of a chemical microreactor.[8] Such reactors can self-organize even for single reactive species (e.g., oxygen in the present case) and are suggested to be dynamic objects. In the case of Fe, the oxidation proceeds through coupled reactions $Fe+O\rightarrow FeO\rightarrow Fe_3O_4+Fe$, followed by $2Fe_3O_4+O\rightarrow 3Fe_2O_3$, wherein the fresh supply of Fe on the surface results from bulk cation diffusion.[12]

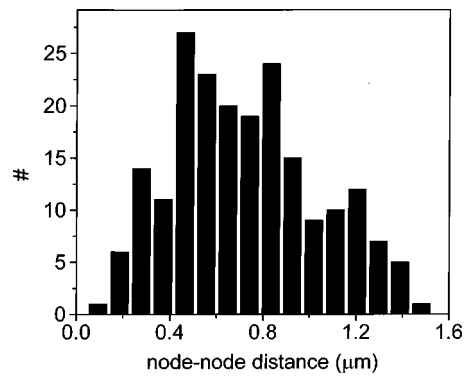

FIG. 5. Node-node length distribution for the polygon patterns in Fig. 1(a).

In order to get some insight into the length scales pertinent to the polygonal patterns, we analyzed the node-node length distribution for the pattern in Fig. 1(a) and the same is shown in Fig. 5. This is a rather broad distribution centered around a length of about 0.7 μm. This can also be taken as a rough measure of the separation between the lifted surface features (bright contrast) reflecting undulations caused by stress relaxations. This issue of stress relaxation in thin films has been discussed by Thouless[13] in the context of the analysis of crack formation under tensile stress. In our case the stress is compressive due to a lower density of the oxide as compared to the metal, hence the surface undulates instead of forming cracks. The general considerations discussed by Thouless[13] are, however, still applicable. In his analysis, the minimum intercrack (undulation) spacing λ, is given by

$$\lambda=8t\left[1-\sqrt{1-\frac{0.5}{(\sigma\sqrt{t}/k)^2}}\right],$$

where t is the film thickness, σ is the stress, and k is the fracture toughness of the film. Use of the expression for critical stress required to induce a single crack (or undulation) in a film, namely, $0.7k/\sqrt{t}$, in conjugation with the equation above, yields a minimum crack (or undulation) spacing of about eight times the film thickness. Since oxidation is a sequential process, the undulations in our film can be expected to be introduced every time the local stress builds to the value of the critical stress, keeping the mean stress below the critical value. Thus, in our 50-nm thick film, the undulation spacing is expected to be of the order of 0.4 μm or more. This is fairly consistent with the distribution shown in Fig. 5. The process of oxidation being quite complex, however, a much better estimate of lengths is hard to expect from a uniform stress model.

It is now important to discuss the further stages of pattern evolution, from high density of small hillocks, to necklike labyrinth, to a polydisperse distribution of large, isolated

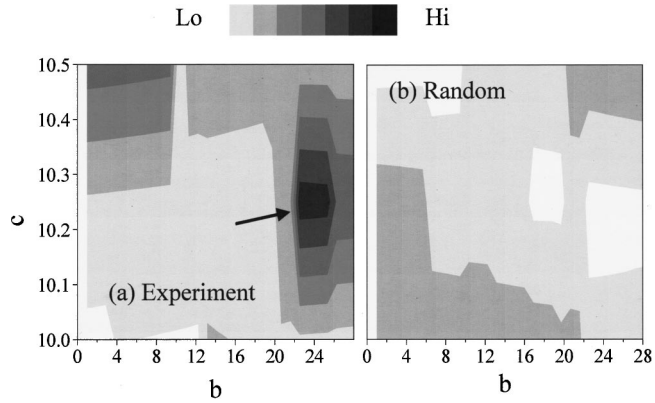

FIG. 6. Results of spiral mapping function $F(b,c)$ for (a) experimental data (image area of 100 μm^2), and (b) computer generated random data points averaged over 4 sets.

hillocks. Drucker[14] has analyzed the influence of elastic energy on the chemical potential and growth rate of diffusionally interacting islands, employing the results derived by Jesser and Kuhlmann-Wisdorf,[15] for equilibrium strain energy in supported clusters. His work suggests a significant role of elastic energy in the late stages of microstructural evolution (Ostwald ripening) in strained systems. In another study, Schuster *et al.*[16] have identified the influence of stress on step kinetics in the ripening process. It is suggested that the steps at the bottom of different islands repel each other due to stress in the connecting film, while the steps at the edges of each isolated relaxed island bunch together causing hillock shapes of islands. The hemispherical shapes of our final hillocks and their narrow size distribution indicate a strong role of stress in the process and seem to have all the features of stress-controlled Ostwald ripening.[17] For the ripening to occur however, a diffusion mechanism is needed to transport atoms between islands. Processes such as self-diffusion involving vacancy motion[18] or coarsening of vacancy clusters[19] have been suggested in this context. Interestingly, for the case of annealing at 1050 °C for 4 h, the data on Fe diffusion in Fe_2O_3 (Ref. 12) gives the diffusion length $\sqrt{Dt}$ of $\sim$0.5 μm. This is comparable to the characteristic lengths of the hillock geometry in Fig. 1(e), indicating a scenario of coarsening by transport and reaction of Fe. X-ray diffraction data show that in the course of raising the temperature, the film is fully oxidized by the time $T\sim 500$ °C is reached. However, in view of its inability to follow the combined chemical-strain equilibrium, the film accepts strain inhomogeneities and vacancy concentrations. The ripening mechanism then operates under inhomogeneous stress fields leading to further morphology development.

The spiral organization of the final hillock assembly [Fig. 1(e)] is interesting. In our case, the island ripening process appears to wind as a spiral under stress fields. The spiral pattern can be characterized by seeking a correlation between the observed pattern and an ideal Euclidean spiral. The equation of an ideal Euclidean spiral in polar coordinates (r,θ) is written as

$$\theta=(cr+b)\mathrm{mod}(2\pi)-\pi \quad \text{for the range} -\pi\leqslant\theta\leqslant\pi.$$

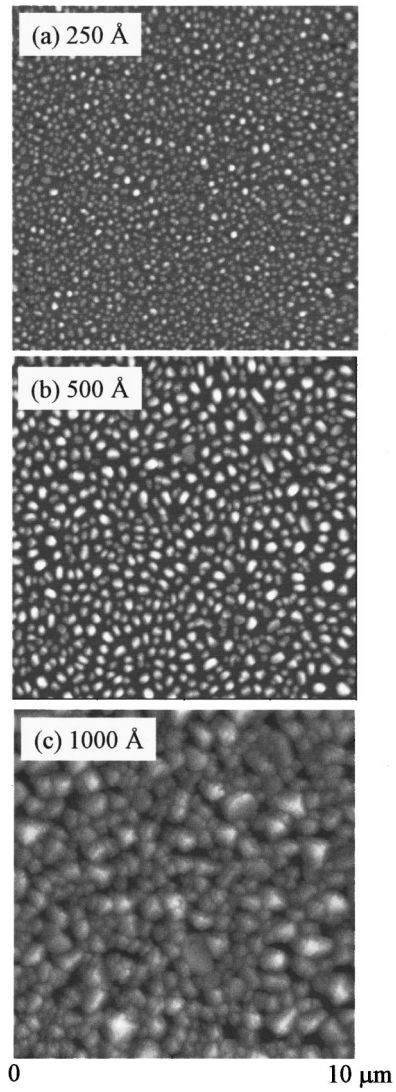

FIG. 7. AFM images (10×10 μm^2) of (a) 250, (b) 500, and (c) 1000 Å Fe-films oxidized at 1050 °C for 4 h.

Note that $2\pi/c$ is the pitch and b is the initial rotation of the spiral. We obtain a correlation function between the data and the ideal spiral for various values of b,c

$$F(c,b)=\sum_i \theta_i^{\mathrm{data}}\theta_{b,c}^{\mathrm{ideal}}(r_i^{\mathrm{data}}),$$

We then obtain the peak of the function $F(c,b)$ to detect the best-fit equation for the observed spiral pattern. Such a correlation was good to within 15% for the experimental data around different centroids of spirals. The comparison of the spiral correlation function for our experimental data, and that for a random arrangement of points generated using a random number generator over comparable length scale (averaged over four datasets), is given in Fig. 6. The arrow in Fig. 6(a) points to the best-fit values of (b,c). No specific correlation is seen for the case in Fig. 6(b).

In the accompanying paper Paper II,[7] the case of oxidation of iron thin film is modeled as a reaction-diffusion system. When the process of Ostwald ripening is not included in

the simulation, leaflike patterns similar to those obtained experimentally for the films oxidized at lower temperature ($<1000\,°C$), are indeed obtained. Since the diffusion lengths at these temperatures are very small (inset of Fig. 3), the ripening mechanism is not expected to be dominant under such conditions. However, when the Ostwald ripening process is included in the simulation, the leaflike pattern are seen to transform into fully developed hillock pattern through different stages (Fig. 4 of Paper II),[7] as observed in our experiments. Interestingly, these patterns also show the spiral coordination of the hillocks (Fig. 5 of Paper II),[7] which is suggested to result from a greater stability of spiral distribution against stress deformation (Paper II).

Figure 7 compares the patterns obtained after the oxidation of Fe films (at $1050\,°C/4h$) having different thickness. In the thinnest film the hillocks are significantly smaller in size. This is because the small amount of available Fe is consumed quickly, and the connectivity between the hillocks is lost in the early stages of pattern evolution. This prohibits the diffusional interactivity and further growth of isolated hillocks. On the other hand, due to larger amount of Fe in the thicker films, the isolated hillocks are not observed in the films having thickness more than about 1000 Å.

We also studied the pattern formation for the Fe films deposited on different substrates such as $LaAlO_3$, Al_2O_3, and $Gd_3Ga_5O_{12}$. The patterns obtained on these surfaces are very similar to those reported here. This indicates that the substrate does not play any major role in the pattern formation.

IV. CONCLUSION

In conclusion, interesting morphology evolutions are observed in thin films of iron subjected to high-temperature thermal oxidation. Small scale and large scale structures are found to evolve under inhomogeneous stress fields. The possible roles of chemical microreactors, bulk diffusion, and Ostwald ripening are discussed. Distributed spiral configurations are observed in films processed at high temperatures.

ACKNOWLEDGMENTS

This work was supported by NSF-MRSEC under Grant No. DMR-00-80008.

*Email address: shinde@squid.umd.edu.
†Email address: ogale@squid.umd.edu
‡On leave from Physical and Technical Research Institute, University of Nizhny Novgorod, 603600, Nizhny Novgorod, Gagarin Ave. 23/3, Russia.

[1] Philip Ball, *The Self-Made Tapestry: Pattern Formation in Nature* (Oxford University, Oxford, 1998).
[2] M. Seul and D. Andelman, Science **267**, 476 (1995).
[3] V. A. Shchukin and D. Bimberg, Rev. Mod. Phys. **71**, 1125 (1999).
[4] J. Tersoff, C. Teichert, and M. G. Lagally, Phys. Rev. Lett. **76**, 1675 (1996) and references therein.
[5] A. K. Horváth, M. Dolnik, A. P. Muñuzuri, A. M. Zhabotinsky, and I. R. Epstein, Phys. Rev. Lett. **83**, 2950 (1999).
[6] S. Aggarwal, A. P. Monga, S. R. Perusse, R. Ramesh, V. Ballarotto, E. D. Williams, B. R. Chalamala, Y. Wei, and R. H. Reuss, Science **287**, 2235 (2000).
[7] Abhijit S. Ogale, Phys. Rev. B **64**, 035409 (2001), referred to as Paper II.
[8] M. Hildebrand, M. Kuperman, H. Wio, A. S. Mikhailov, and G. Ertl, Phys. Rev. Lett. **83**, 1475 (1999).
[9] B. J. Spencer, P. W. Voorhees, and S. H. Davis, Phys. Rev. Lett. **67**, 3696 (1991).
[10] P. Hanesch and E. Bertel, Phys. Rev. Lett. **79**, 1523 (1997).
[11] J. Müller and M. Grant, Phys. Rev. Lett. **82**, 1736 (1999).
[12] Kubaschewski and Hopkins, *Oxidation of Metals and Alloys* (Butterworths, London, 1967).
[13] M. D. Thouless, J. Am. Ceram. Soc. **73**, 2144 (1990).
[14] J. Drucker, Phys. Rev. B **48**, 18 203 (1993).
[15] W. A. Jesser and D. Kuhlmann-Wisdorf, Phys. Status Solidi **19**, 95 (1967).
[16] R. Schuster, H. Roder, K. Bromann, H. Brune, and K. Kern, Phys. Rev. B **54**, 13 476 (1996).
[17] J. A. Floro, M. B. Sinclair, E. Chason, L. B. Freund, R. D. Tweston, R. Q. Hwang, and G. A. Lucadamo, Phys. Rev. Lett. **84**, 701 (2000).
[18] J. B. Hannon, C. Klunker, M. Giesen, and H. Ibach, Phys. Rev. Lett. **79**, 2506 (1997).
[19] J.-M. Wen, J. W. Evans, M. C. Bartelt, J. W. Burnett, and P. A. Thiel, Phys. Rev. Lett. **76**, 652 (1996).